

1 A comparison of nine machine learning mutagenicity models
2 and their application for predicting pyrrolizidine alkaloids

3 Christoph Helma^{*1}, Verena Schöning⁵, Jürgen Drewe^{2,4}, and Philipp Boss³

4 ¹in silico toxicology gmbh, Rastatterstrasse 41, 4057 Basel, Switzerland

5 ²Max Zeller Söhne AG, Seeblickstrasse 4, 8590 Romanshorn, Switzerland

6 ³Berlin Institute for Medical Systems Biology, Max Delbrück Center for Molecular
7 Medicine in the Helmholtz Association, Robert-Rössle-Strasse 10, Berlin, 13125, Germany

8 ⁴Clinical Pharmacology, Department of Pharmaceutical Sciences, University Hospital
9 Basel, University of Basel, Petersgraben 4, 4031 Basel, Switzerland

10 ⁵Clinical Pharmacology and Toxicology, Department of General Internal Medicine,
11 University Hospital Bern, University of Bern, Inselspital, 3010 Bern, Switzerland

12 ^{*} Correspondence: Christoph Helma <helma@in-silico.ch>

13 Random forest, support vector machine, logistic regression, neural
14 networks and k-nearest neighbor (**lazar**) algorithms, were applied to new
15 *Salmonella* mutagenicity dataset with 8290 unique chemical structures
16 utilizing MolPrint2D and Chemistry Development Kit (CDK) descriptors.
17 Crossvalidation accuracies of all investigated models ranged from 80-85%
18 which is comparable with the interlaboratory variability of the *Salmonella*
19 mutagenicity assay. Pyrrolizidine alkaloid predictions showed a clear
20 distinction between chemical groups, where Otonecines had the highest
21 proportion of positive mutagenicity predictions and Monoester the lowest.

22 Introduction

23 **TODO:** rationale for investigation

24 The main objectives of this study were

- 25 • to generate a new mutagenicity training dataset, by combining the most compre-
26 hensive public datasets
- 27 • to compare the performance of MolPrint2D (*MP2D*) fingerprints with Chemistry
28 Development Kit (*CDK*) descriptors
- 29 • to compare the performance of global QSAR models (random forests (*RF*), support
30 vector machines (*SVM*), logistic regression (*LR*), neural nets (*NN*)) with local
31 models (*lazar*)
- 32 • to apply these models for the prediction of pyrrolizidine alkaloid mutagenicity

33 Materials and Methods

34 Data

35 Mutagenicity training data

36 An identical training dataset was used for all models. The training dataset was compiled
37 from the following sources:

- 38 • Kazius/Bursi Dataset (4337 compounds, Kazius, McGuire, and Bursi (2005)):
39 http://cheminformatics.org/datasets/bursi/cas_4337.zip
- 40 • Hansen Dataset (6513 compounds, Hansen et al. (2009)): [http://doc.ml.tu-berlin.
41 de/toxbenchmark/Mutagenicity_N6512.csv](http://doc.ml.tu-berlin.de/toxbenchmark/Mutagenicity_N6512.csv)
- 42 • EFSA Dataset (695 compounds EFSA (2016)): [https://data.europa.eu/euodp/
43 data/storage/f/2017-0719T142131/GENOTOX%20data%20and%20dictionary.xls](https://data.europa.eu/euodp/data/storage/f/2017-0719T142131/GENOTOX%20data%20and%20dictionary.xls)

44 Mutagenicity classifications from Kazius and Hansen datasets were used without further
45 processing. To achieve consistency with these datasets, EFSA compounds were classified
46 as mutagenic, if at least one positive result was found for TA98 or T100 Salmonella
47 strains.

48 Dataset merges were based on unique SMILES (*Simplified Molecular Input Line En-*
49 *try Specification*, Weininger, Weininger, and Weininger (1989)) strings of the compound
50 structures. Duplicated experimental data with the same outcome was merged into a
51 single value, because it is likely that it originated from the same experiment. Contradic-
52 tory results were kept as multiple measurements in the database. The combined training
53 dataset contains 8290 unique structures and 8309 individual measurements.

54 Source code for all data download, extraction and merge operations is pub-
55 licly available from the git repository <https://git.in-silico.ch/mutagenicity-paper>
56 under a GPL3 License. The new combined dataset can be found at <https://git.in-silico.ch/mutagenicity-paper/tree/mutagenicity/mutagenicity.csv>.

58 **Pyrrolizidine alkaloid (PA) dataset**

59 The pyrrolizidine alkaloid dataset was created from five independent, necine base sub-
60 structure searches in PubChem (<https://pubchem.ncbi.nlm.nih.gov/>) and compared to
61 the PAs listed in the EFSA publication EFSA (2011) and the book by Mattocks Mattocks
62 (1986), to ensure, that all major PAs were included. PAs mentioned in these publica-
63 tions which were not found in the downloaded substances were searched individually
64 in PubChem and, if available, downloaded separately. Non-PA substances, duplicates,
65 and isomers were removed from the files, but artificial PAs, even if unlikely to occur in
66 nature, were kept. The resulting PA dataset comprised a total of 602 different PAs.

67 The PAs in the dataset were classified according to structural features. A total of 9
68 different structural features were assigned to the necine base, modifications of the necine

69 base and to the necic acid:

70 For the necine base, the following structural features were chosen:

- 71 • Retronecine-type (1,2-unsaturated necine base, 392 compounds)
- 72 • Otonecine-type (1,2-unsaturated necine base, 46 compounds)
- 73 • Platyneccine-type (1,2-saturated necine base, 140 compounds)

74 For the modifications of the necine base, the following structural features were chosen:

- 75 • N-oxide-type (84 compounds)
- 76 • Tertiary-type (PAs which were neither from the N-oxide- nor DHP-type, 495 com-
77 pounds)
- 78 • Dehydropyrrolizidine-type (pyrrolic ester, 23 compounds)

79 For the necic acid, the following structural features were chosen:

- 80 • Monoester-type (154 compounds)
- 81 • Open-ring diester-type (163 compounds)
- 82 • Macrocyclic diester-type (255 compounds)

83 The compilation of the PA dataset is described in detail in Schöning et al. (2017).

84 **Descriptors**

85 **MolPrint2D (MP2D) fingerprints**

86 MolPrint2D fingerprints (O’Boyle et al. (2011)) use atom environments as molecular
87 representation. They determine for each atom in a molecule, the atom types of its
88 connected atoms to represent their chemical environment. This resembles basically the
89 chemical concept of functional groups.

90 In contrast to predefined lists of fragments (e.g. FP3, FP4 or MACCs fingerprints) or
91 descriptors (e.g CDK) they are generated dynamically from chemical structures. This

92 has the advantage that they can capture unknown substructures of toxicological relevance
93 that are not included in other descriptors. In addition they allow the efficient calculation
94 of chemical similarities (e.g. Tanimoto indices) with simple set operations.

95 MolPrint2D fingerprints were calculated with the OpenBabel cheminformatics library
96 (O’Boyle et al. (2011)). They can be obtained from the following locations:

97 *Training data:*

- 98 • sparse representation ([https://git.in-silico.ch/mutagenicity-paper/tree/mutagenicity/
99 mp2d/fingerprints.mp2d](https://git.in-silico.ch/mutagenicity-paper/tree/mutagenicity/mp2d/fingerprints.mp2d))
- 100 • descriptor matrix ([https://git.in-silico.ch/mutagenicity-paper/tree/mutagenicity/
101 mp2d/mutagenicity-fingerprints.csv.gz](https://git.in-silico.ch/mutagenicity-paper/tree/mutagenicity/mp2d/mutagenicity-fingerprints.csv.gz))

102 *Pyrrrolizidine alkaloids:*

- 103 • sparse representation ([https://git.in-silico.ch/mutagenicity-paper/tree/pyrrolizidine-alkaloids/
104 mp2d/fingerprints.mp2d](https://git.in-silico.ch/mutagenicity-paper/tree/pyrrolizidine-alkaloids/mp2d/fingerprints.mp2d))
- 105 • descriptor matrix ([https://git.in-silico.ch/mutagenicity-paper/tree/pyrrolizidine-alkaloids/
106 mp2d/pa-fingerprints.csv.gz](https://git.in-silico.ch/mutagenicity-paper/tree/pyrrolizidine-alkaloids/mp2d/pa-fingerprints.csv.gz))

107 **Chemistry Development Kit (CDK) descriptors**

108 Molecular 1D and 2D descriptors were calculated with the PaDEL-Descriptors program
109 (<http://www.yapcsoft.com> version 2.21, Yap (2011)). PaDEL uses the Chemistry De-
110 velopment Kit (CDK, <https://cdk.github.io/index.html>) library for descriptor calcula-
111 tions.

112 As the training dataset contained 8290 instances, it was decided to delete instances
113 with missing values during data pre-processing. Furthermore, substances with equivocal
114 outcome were removed. The final training dataset contained 1442 descriptors for 8083
115 compounds.

116 CDK training data can be obtained from [https://git.in-silico.ch/mutagenicity-paper/
117 tree/mutagenicity/cdk/mutagenicity-mod-2.new.csv](https://git.in-silico.ch/mutagenicity-paper/tree/mutagenicity/cdk/mutagenicity-mod-2.new.csv).

118 The same procedure was applied for the pyrrolizidine dataset yielding descriptors for
119 compounds. CDK features for pyrrolizidine alkaloids are available at [https://git.in-silico.
120 ch/mutagenicity-paper/tree/pyrrolizidine-alkaloids/cdk/PA-Padel-2D_m2.csv](https://git.in-silico.ch/mutagenicity-paper/tree/pyrrolizidine-alkaloids/cdk/PA-Padel-2D_m2.csv).

121 **Algorithms**

122 **lazar**

123 **lazar** (*lazy structure activity relationships*) is a modular framework for read-across model
124 development and validation. It follows the following basic workflow: For a given chemical
125 structure **lazar**:

- 126 • searches in a database for similar structures (neighbours) with experimental data,
- 127 • builds a local QSAR model with these neighbours and
- 128 • uses this model to predict the unknown activity of the query compound.

129 This procedure resembles an automated version of read across predictions in toxicology,
130 in machine learning terms it would be classified as a k-nearest-neighbour algorithm.

131 Apart from this basic workflow, **lazar** is completely modular and allows the researcher to
132 use arbitrary algorithms for similarity searches and local QSAR (*Quantitative structure–
133 activity relationship*) modelling. Algorithms used within this study are described in the
134 following sections.

135 **Feature preprocessing**

136 MolPrint2D features were used without preprocessing. Near zero variance and strongly
137 correlated CDK descriptors were removed and the remaining descriptor values were

138 centered and scaled. Preprocessing was performed with the R `caret` `preProcess` function
139 using the methods “nzv”, “corr”, “center” and “scale” with default settings.

140 **Neighbour identification**

141 Utilizing this modularity, similarity calculations were based both on MolPrint2D finger-
142 prints and on CDK descriptors.

143 For MolPrint2D fingerprints chemical similarity between two compounds a and b is
144 expressed as the proportion between atom environments common in both structures
145 $A \cap B$ and the total number of atom environments $A \cup B$ (Jaccard/Tanimoto index).

$$sim = \frac{|A \cap B|}{|A \cup B|}$$

146 For CDK descriptors chemical similarity between two compounds a and b is expressed
147 as the cosine similarity between the descriptor vectors A for a and B for b .

$$sim = \frac{A \cdot B}{|A||B|}$$

148 Threshold selection is a trade-off between prediction accuracy (high threshold) and the
149 number of predictable compounds (low threshold). As it is in many practical cases
150 desirable to make predictions even in the absence of closely related neighbours, we follow
151 a tiered approach:

- 152 • First a similarity threshold of 0.5 (MP2D/Tanimoto) or 0.9 (CDK/Cosine) is used
153 to collect neighbours, to create a local QSAR model and to make a prediction for
154 the query compound. This are predictions with *high confidence*.
- 155 • If any of these steps fails, the procedure is repeated with a similarity threshold of
156 0.2 (MP2D/Tanimoto) or 0.7 (CDK/Cosine) and the prediction is flagged with a

157 warning that it might be out of the applicability domain of the training data (*low*
158 *confidence*).

- 159 • These Similarity thresholds are the default values chosen by software developers
160 and remained unchanged during the course of these experiments.

161 Compounds with the same structure as the query structure are automatically eliminated
162 from neighbours to obtain unbiased predictions in the presence of duplicates.

163 **Local QSAR models and predictions**

164 Only similar compounds (neighbours) above the threshold are used for local QSAR
165 models. In this investigation, we are using a weighted majority vote from the neigh-
166 bour's experimental data for mutagenicity classifications. Probabilities for both classes
167 (mutagenic/non-mutagenic) are calculated according to the following formula and the
168 class with the higher probability is used as prediction outcome.

$$p_c = \frac{\sum \text{sim}_{n,c}}{\sum \text{sim}_n}$$

169 p_c Probability of class c (e.g. mutagenic or non-mutagenic)

170 $\sum \text{sim}_{n,c}$ Sum of similarities of neighbours with class c

171 $\sum \text{sim}_n$ Sum of all neighbours

172 **Applicability domain**

173 The applicability domain (AD) of **lazar** models is determined by the structural diver-
174 sity of the training data. If no similar compounds are found in the training data no
175 predictions will be generated. Warnings are issued if the similarity threshold had to be
176 lowered from 0.5 to 0.2 in order to enable predictions. Predictions without warnings
177 can be considered as close to the applicability domain (*high confidence*) and predictions

178 with warnings as more distant from the applicability domain (*low confidence*). Quantita-
179 tive applicability domain information can be obtained from the similarities of individual
180 neighbours.

181 **Validation**

182 10-fold cross validation was performed for model evaluation.

183 **Pyrrolizidine alkaloid predictions**

184 For the prediction of pyrrolizidine alkaloids models were generated with the MP2D and
185 CDK training datasets. The complete feature set was used for MP2D predictions, for
186 CDK predictions the intersection between training and pyrrolizidine alkaloid features
187 was used.

188 **Availability**

- 189 • Source code for this manuscript (GPL3): [https://git.in-silico.ch/lazar/tree/?h=](https://git.in-silico.ch/lazar/tree/?h=mutagenicity-paper)
190 [mutagenicity-paper](https://git.in-silico.ch/lazar/tree/?h=mutagenicity-paper)
- 191 • Crossvalidation experiments (GPL3): [https://git.in-silico.ch/lazar/tree/models/](https://git.in-silico.ch/lazar/tree/models/?h=mutagenicity-paper)
192 [?h=mutagenicity-paper](https://git.in-silico.ch/lazar/tree/models/?h=mutagenicity-paper)
- 193 • Pyrrolizidine alkaloid predictions (GPL3): [https://git.in-silico.ch/lazar/tree/](https://git.in-silico.ch/lazar/tree/predictions/?h=mutagenicity-paper)
194 [predictions/?h=mutagenicity-paper](https://git.in-silico.ch/lazar/tree/predictions/?h=mutagenicity-paper)
- 195 • Public web interface: <https://lazar.in-silico.ch>

196 **Tensorflow models**

197 **Feature Preprocessing**

198 For preprocessing of the CDK features we used a quantile transformation to a uniform
199 distribution. MP2D features were not preprocessed.

200 **Random forests (*RF*)**

201 For the random forest classifier we used the parameters `n_estimators=1000` and
202 `max_leaf_nodes=200`. For the other parameters we used the scikit-learn default values.

203 **Logistic regression (SGD) (*LR-sgd*)**

204 For the logistic regression we used an ensemble of five trained models. For each model
205 we used a batch size of 64 and trained for 50 epoch. As an optimizer ADAM was chosen.
206 For the other parameters we used the tensorflow default values.

207 **Logistic regression (scikit) (*LR-scikit*)**

208 For the logistic regression we used as parameters the scikit-learn default values.

209 **Neural Nets (*NN*)**

210 For the neural network we used an ensemble of five trained models. For each model we
211 used a batch size of 64 and trained for 50 epoch. As an optimizer ADAM was chosen.
212 The neural network had 4 hidden layers with 64 nodes each and a ReLu activation
213 function. For the other parameters we used the tensorflow default values.

214 **Support vector machines (*SVM*)**

215 We used the SVM implemented in scikit-learn. We used the parameters `kernel='rbf'`,
216 `gamma='scale'`. For the other parameters we used the scikit-learn default values.

217 **Validation**

218 10-fold cross-validation was used for all Tensorflow models.

219 **Pyrrolizidine alkaloid predictions**

220 For the prediction of pyrrolizidine alkaloids we trained the model described above on
221 the training data. For training and prediction only the features were used that were in
222 the intersection of features from the training data and the pyrrolizidine alkaloids.

223 **Availability**

224 Jupyter notebooks for these experiments can be found at the following locations

225 *Crossvalidation:*

- 226 • MolPrint2D fingerprints: [https://git.in-silico.ch/mutagenicity-paper/tree/
227 crossvalidations/mp2d/tensorflow](https://git.in-silico.ch/mutagenicity-paper/tree/crossvalidations/mp2d/tensorflow)
- 228 • CDK descriptors: [https://git.in-silico.ch/mutagenicity-paper/tree/crossvalidations/
229 cdk/tensorflow](https://git.in-silico.ch/mutagenicity-paper/tree/crossvalidations/cdk/tensorflow)

230 *Pyrrolizidine alkaloids:*

- 231 • MolPrint2D fingerprints: [https://git.in-silico.ch/mutagenicity-paper/tree/
232 pyrrolizidine-alkaloids/mp2d/tensorflow](https://git.in-silico.ch/mutagenicity-paper/tree/pyrrolizidine-alkaloids/mp2d/tensorflow)
- 233 • CDK descriptors: [https://git.in-silico.ch/mutagenicity-paper/tree/pyrrolizidine-alkaloids/
234 cdk/tensorflow](https://git.in-silico.ch/mutagenicity-paper/tree/pyrrolizidine-alkaloids/cdk/tensorflow)
- 235 • CDK desc

236 Results

237 10-fold crossvalidations

238 Crossvalidation results are summarized in the following tables: Table 1 shows results
239 with MolPrint2D descriptors and Table 2 with CDK descriptors.

Table 1: Summary of crossvalidation results with MolPrint2D descriptors (lazar-HC: lazar with high confidence, lazar-all: all lazar predictions, RF: random forests, LR-sgd: logistic regression (stochastic gradient descent), LR-scikit: logistic regression (scikit), NN: neural networks, SVM: support vector machines)

	lazar-HC	lazar-all	RF	LR-sgd	LR-scikit	NN	SVM
Accuracy	84	82	80	84	84	84	84
True positive rate	89	85	78	83	83	82	83
True negative rate	78	78	82	84	85	85	86
Positive predictive value	83	80	81	84	84	84	85
Negative predictive value	86	84	80	84	84	83	84
Nr. predictions	5864	7782	8303	8303	8303	8303	8303

Table 2: Summary of crossvalidation results with CDK descriptors (lazar-HC: lazar with high confidence, lazar-all: all lazar predictions, RF: random forests, LR-sgd: logistic regression (stochastic gradient descent), LR-scikit: logistic regression (scikit), NN: neural networks, SVM: support vector machines)

	lazar-HC	lazar-all	RF	LR-sgd	LR-scikit	NN	SVM
Accuracy	85	82	84	79	80	85	82
True positive rate	87	84	81	81	80	85	82
True negative rate	82	80	86	78	80	85	82
Positive predictive value	85	81	85	79	80	85	82
Negative predictive value	85	82	82	80	80	85	82

	lazar-HC	lazar-all	RF	LR-sgd	LR-scikit	NN	SVM
Nr. predictions	4872	7353	8077	8077	8077	8077	8077

240 Figure 1 depicts the position of all crossvalidation results in receiver operating charac-
 241 teristic (ROC) space.

242 Confusion matrices for all models are available from the git repository [https://git.in-](https://git.in-silico.ch/mutagenicity-paper/tree/crossvalidations/confusion-matrices/)
 243 [silico.ch/mutagenicity-paper/tree/crossvalidations/confusion-matrices/](https://git.in-silico.ch/mutagenicity-paper/tree/crossvalidations/confusion-matrices/), individual pre-
 244 dictions can be found in <https://git.in-silico.ch/mutagenicity-paper/tree/crossvalidations/predictions/>.

245 All investigated algorithm/descriptor combinations give accuracies between (80 and 85%)
 246 which is equivalent to the experimental variability of the *Salmonella typhimurium* mu-
 247 tagenicity bioassay (80-85%, Benigni and Giuliani (1988)). Sensitivities and specificities
 248 are balanced in all of these models.

249 **Pyrrrolizidine alkaloid mutagenicity predictions**

250 Mutagenicity predictions of 602 pyrrolizidine alkaloids (PAs) from all investigated
 251 models can be downloaded from [https://git.in-silico.ch/mutagenicity-paper/tree/](https://git.in-silico.ch/mutagenicity-paper/tree/pyrrolizidine-alkaloids/pa-predictions.csv)
 252 [pyrrolizidine-alkaloids/pa-predictions.csv](https://git.in-silico.ch/mutagenicity-paper/tree/pyrrolizidine-alkaloids/pa-predictions.csv). A visual representation of all PA predictions
 253 can be found at [https://git.in-silico.ch/mutagenicity-paper/tree/pyrrolizidine-alkaloids/](https://git.in-silico.ch/mutagenicity-paper/tree/pyrrolizidine-alkaloids/pa-predictions.pdf)
 254 [pa-predictions.pdf](https://git.in-silico.ch/mutagenicity-paper/tree/pyrrolizidine-alkaloids/pa-predictions.pdf).

255 Figure 2 displays the proportion of positive mutagenicity predictions from all models
 256 for the different pyrrolizidine alkaloid groups. Tensorflow models predicted all 602
 257 pyrrolizidine alkaloids, **lazar** MP2D models predicted 560 compounds (301 with high
 258 confidence) and **lazar** CDK models 500 compounds (246 with high confidence).

259 For the visualisation of the position of pyrrolizidine alkaloids in respect to the train-
 260 ing data set we have applied t-distributed stochastic neighbor embedding (t-SNE,

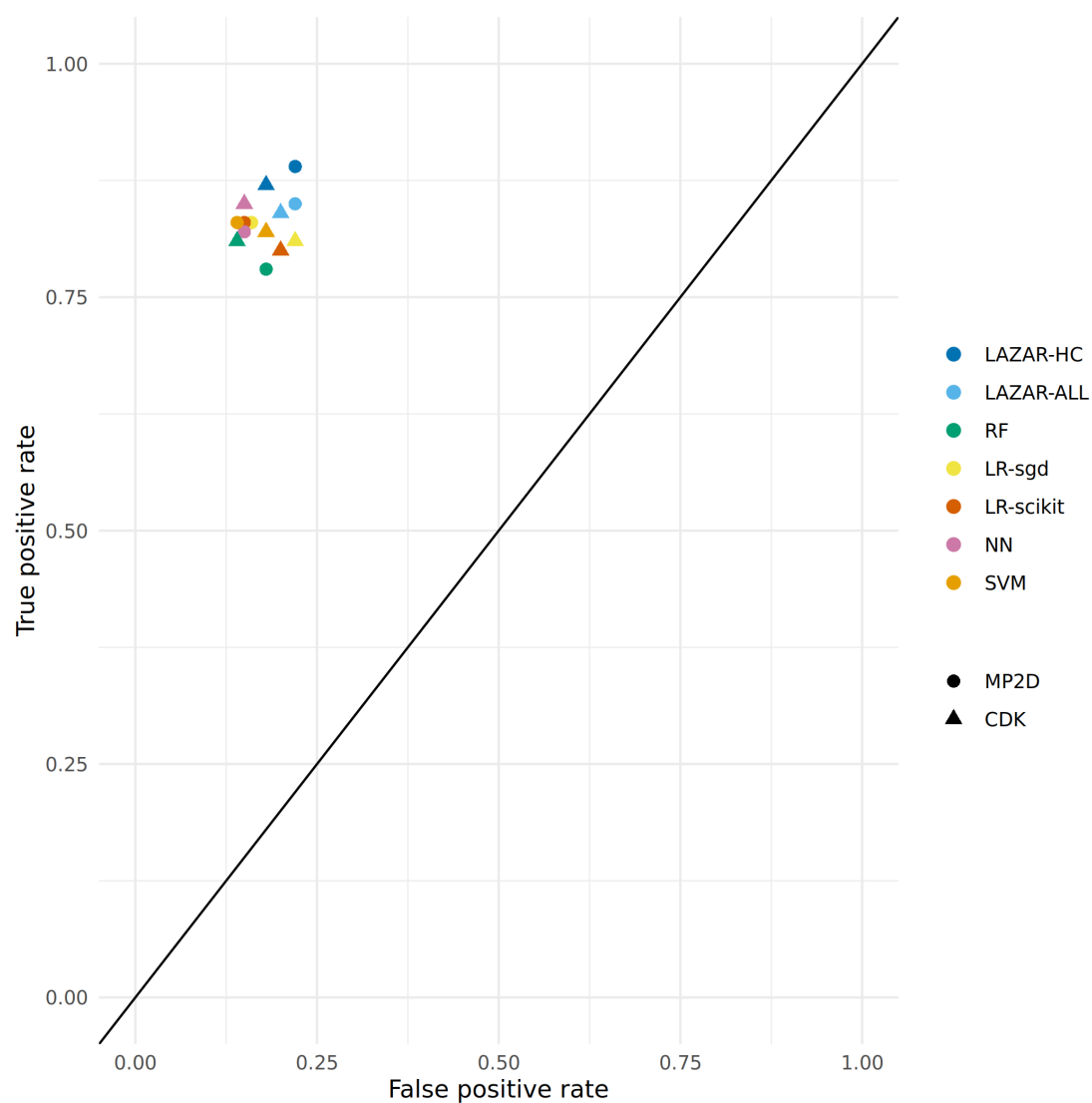


Figure 1: ROC plot of crossvalidation results (lazar-HC: lazar with high confidence, lazar-all: all lazar predictions, RF: random forests, LR-sgd: logistic regression (stochastic gradient descent), LR-scikit: logistic regression (scikit), NN: neural networks, SVM: support vector machines).

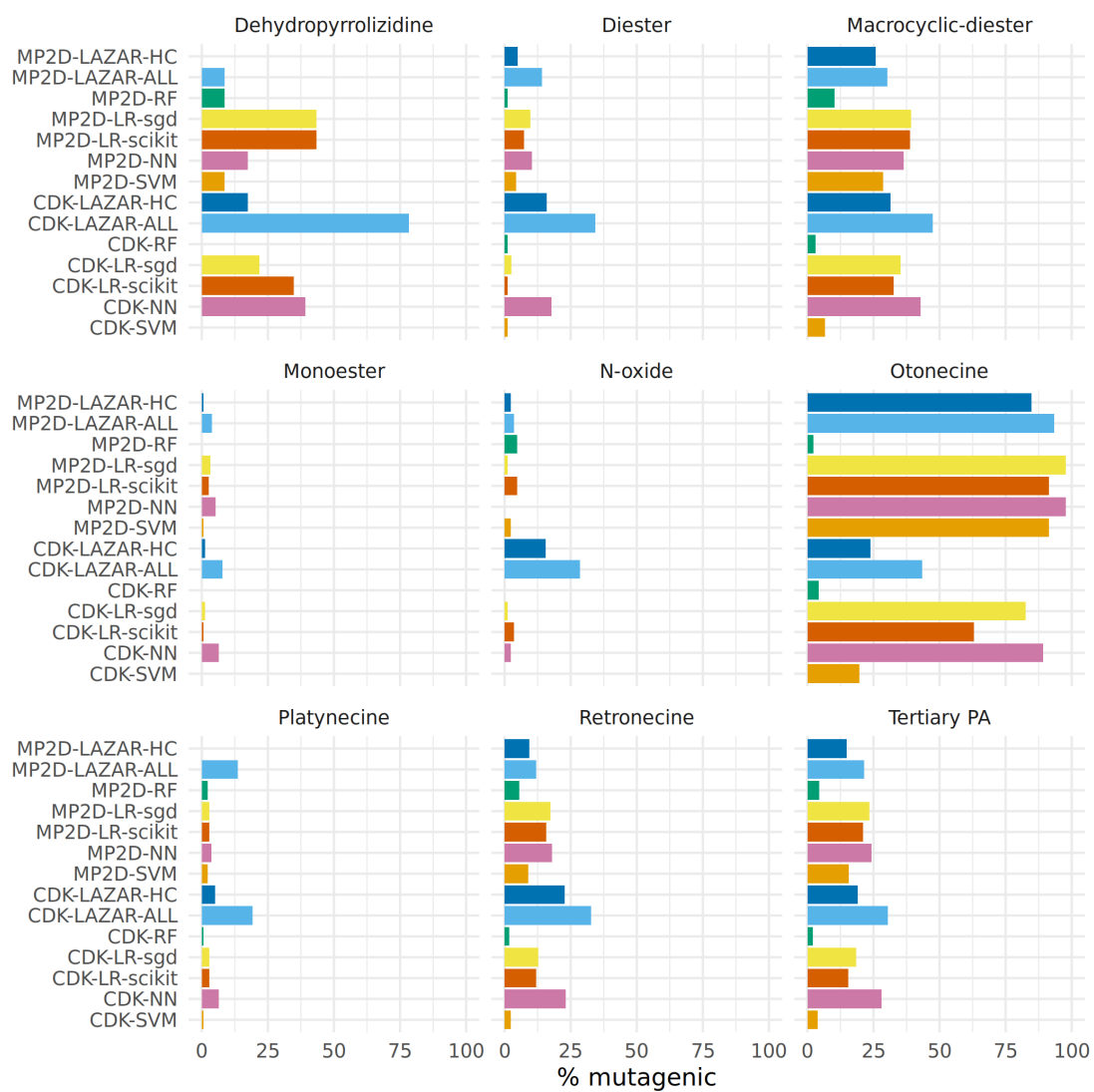


Figure 2: Summary of pyrrolizidine alkaloid predictions

261 Maaten and Hinton (2008)) for MolPrint2D and CDK descriptors. t-SNE maps
262 each high-dimensional object (chemical) to a two-dimensional point, maintaining the
263 high-dimensional distances of the objects. Similar objects are represented by nearby
264 points and dissimilar objects are represented by distant points. t-SNE coordinates were
265 calculated with the R `Rtsne` package using the default settings (perplexity = 30, theta
266 = 0.5, max_iter = 1000).

267 Figure 3 shows the t-SNE of pyrrolizidine alkaloids (PA) and the mutagenicity train-
268 ing data in MP2D space (Tanimoto/Jaccard similarity), which resembles basically the
269 structural diversity of the investigated compounds.

270 Figure 4 shows the t-SNE of pyrrolizidine alkaloids (PA) and the mutagenicity train-
271 ing data in CDK space (Euclidean similarity), which resembles basically the physical-
272 chemical properties of the investigated compounds.

273 Figure 5 and Figure 6 depict two example pyrrolizidine alkaloid mutagenicity predictions
274 in the context of training data. t-SNE visualisations of all investigated models can be
275 downloaded from <https://git.in-silico.ch/mutagenicity-paper/figures>.

276 Discussion

277 Data

278 A new training dataset for *Salmonella* mutagenicity was created from three different
279 sources (Kazius, McGuire, and Bursi (2005), Hansen et al. (2009), EFSA (2016)). It
280 contains 8290 unique chemical structures, which is according to our knowledge the
281 largest public mutagenicity dataset presently available. The new training data can
282 be downloaded from [https://git.in-silico.ch/mutagenicity-paper/tree/mutagenicity/
283 mutagenicity.csv](https://git.in-silico.ch/mutagenicity-paper/tree/mutagenicity/mutagenicity.csv).

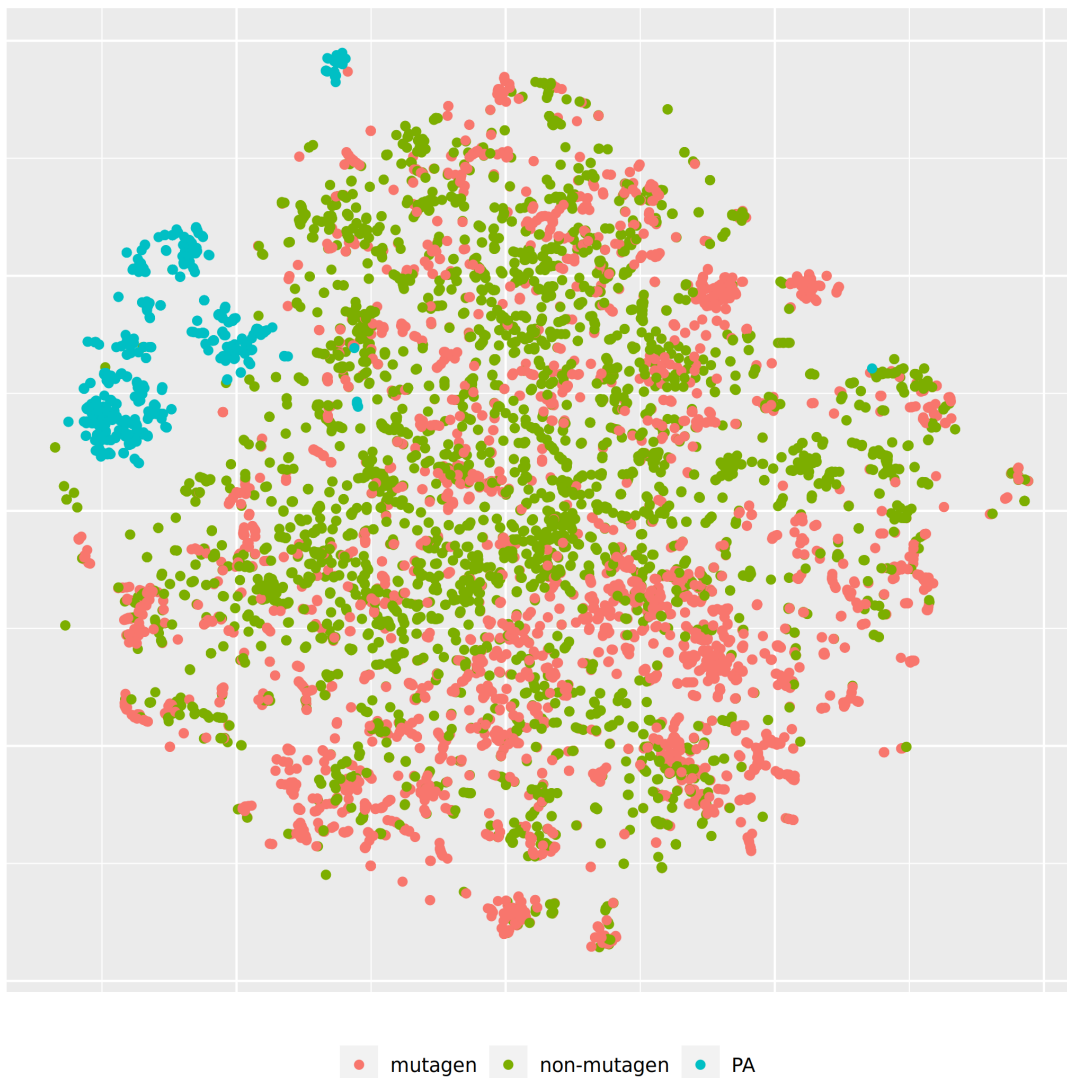


Figure 3: t-SNE visualisation of mutagenicity training data and pyrrolizidine alkaloids (PA) in MP2D space

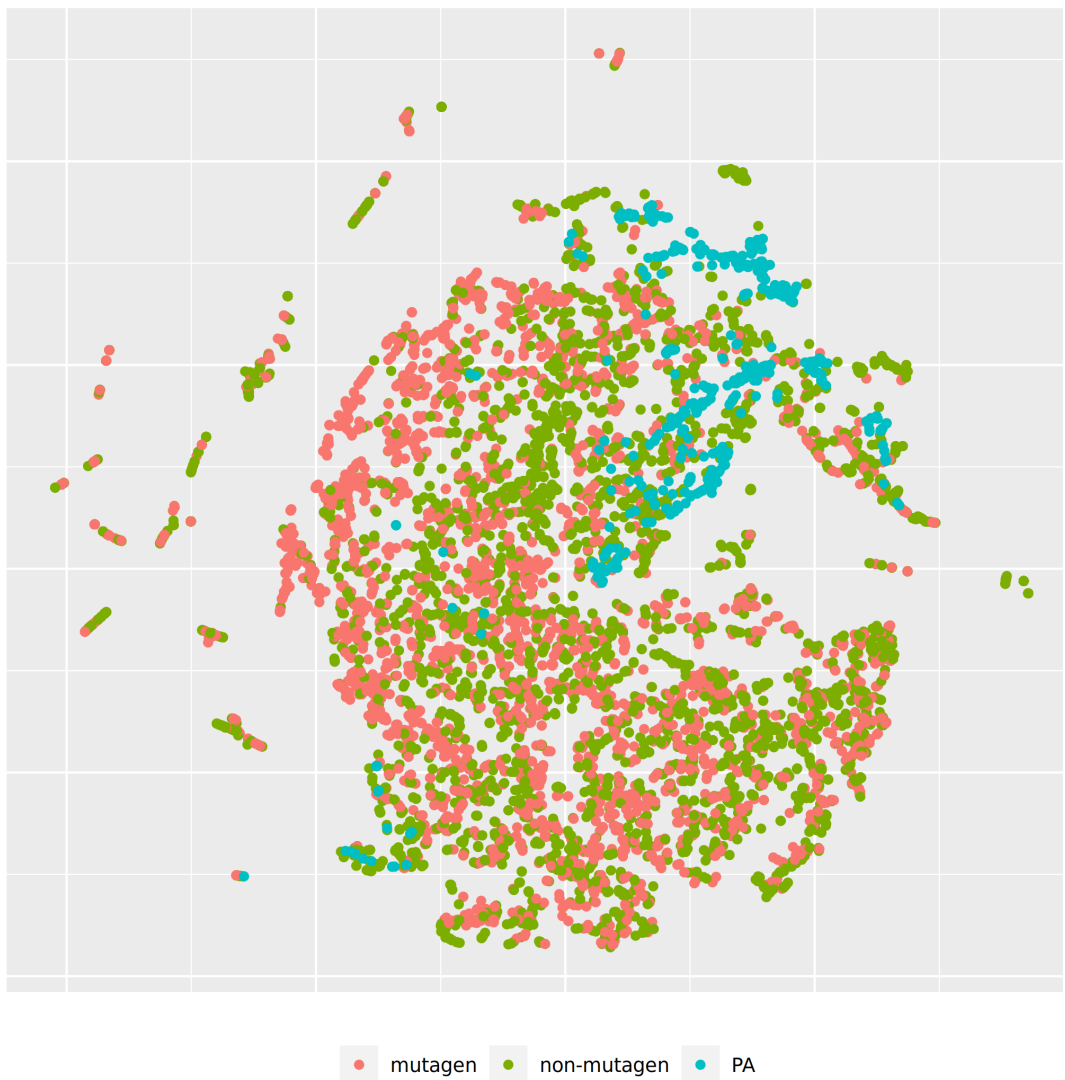


Figure 4: t-SNE visualisation of mutagenicity training data and pyrrolizidine alkaloids (PA) in CDK space

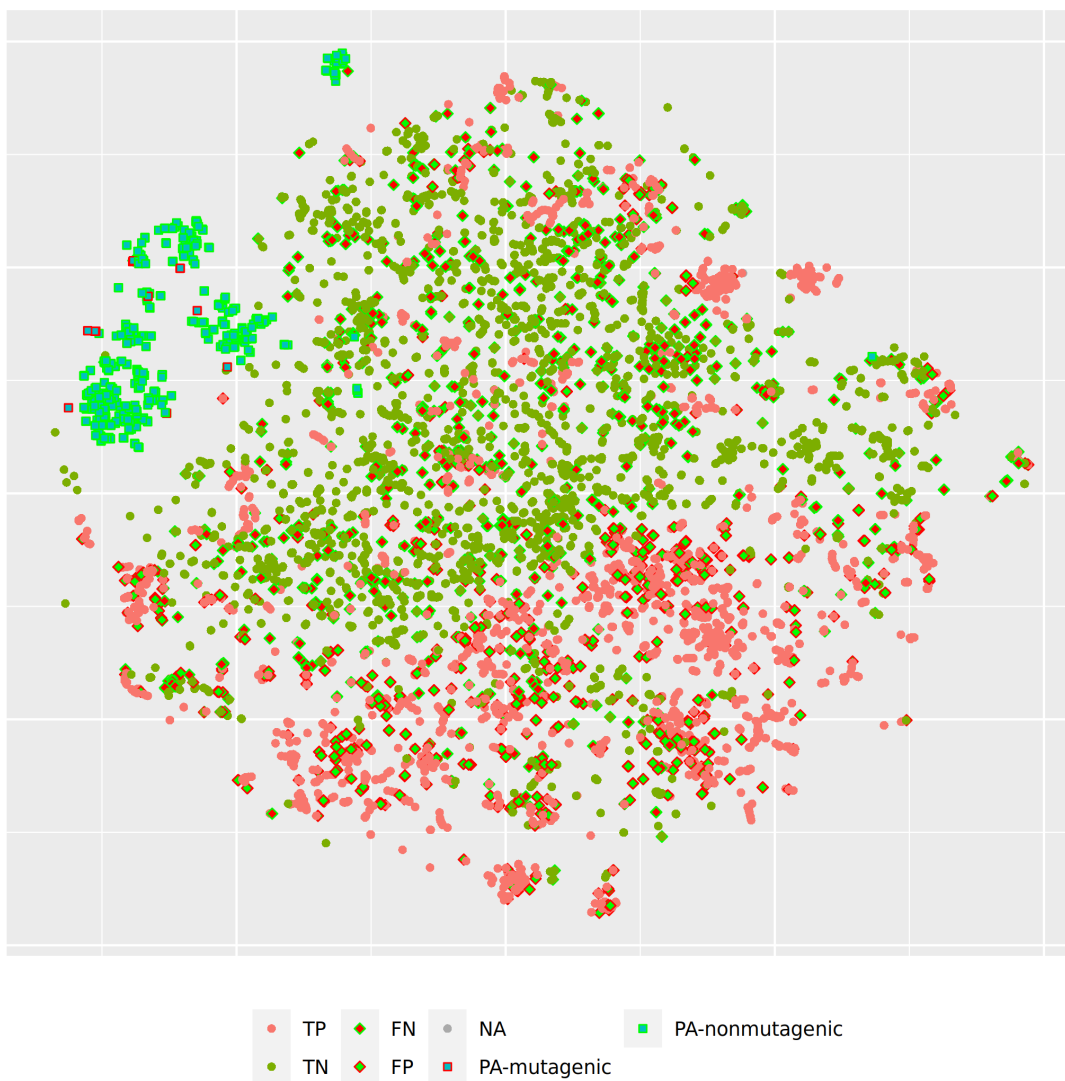


Figure 5: t-SNE visualisation of MP2D random forest predictions

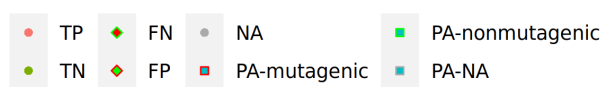
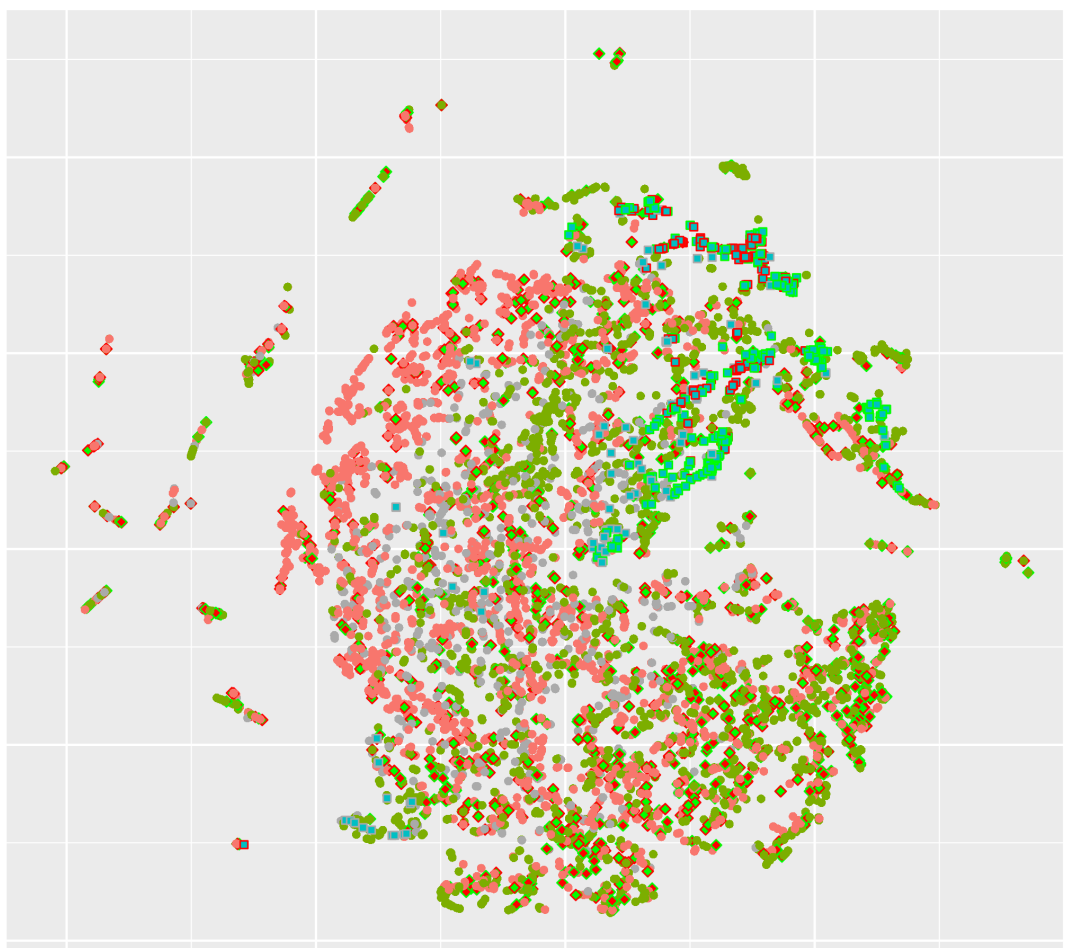


Figure 6: t-SNE visualisation of all CDK lazar predictions

284 Algorithms

285 **lazar** is formally a *k-nearest-neighbor* algorithm that searches for similar structures
286 for a given compound and calculates the prediction based on the experimental data for
287 these structures. The QSAR literature calls such models frequently *local models*, because
288 models are generated specifically for each query compound. The investigated tensorflow
289 models are in contrast *global models*, i.e. a single model is used to make predictions for
290 all compounds. It has been postulated in the past, that local models are more accurate,
291 because they can account better for mechanisms, that affect only a subset of the training
292 data.

293 Table 1, Table 2 and Figure 1 show that the crossvalidation accuracies of all models are
294 comparable to the experimental variability of the *Salmonella typhimurium* mutagenicity
295 bioassay (80-85% according to Benigni and Giuliani (1988)). All of these models have
296 balanced sensitivity (true position rate) and specificity (true negative rate) and provide
297 highly significant concordance with experimental data (as determined by McNemar’s
298 Test). This is a clear indication that *in-silico* predictions can be as reliable as the
299 bioassays. Given that the variability of experimental data is similar to model variability
300 it is impossible to decide which model gives the most accurate predictions, as models
301 with higher accuracies might just approximate experimental errors better than more
302 robust models.

303 Our results do not support the assumption that local models are superior to global
304 models for classification purposes. For regression models (lowest observed effect level)
305 we have found however that local models may outperform global models (Helma et al.
306 (2018)) with accuracies similar to experimental variability.

307 As all investigated algorithms give similar accuracies the selection will depend more on
308 practical considerations than on intrinsic properties. Nearest neighbor algorithms like
309 **lazar** have the practical advantage that the rationales for individual predictions can be

310 presented in a straightforward manner that is understandable without a background in
311 statistics or machine learning (Figure 7). This allows a critical examination of individual
312 predictions and prevents blind trust in models that are intransparent to users with a
313 toxicological background.

314 **Descriptors**

315 This study uses two types of descriptors for the characterisation of chemical structures:
316 *MolPrint2D* fingerprints (MP2D, Bender et al. (2004)) use atom environments (i.e.
317 connected atom types for all atoms in a molecule) as molecular representation, which
318 resembles basically the chemical concept of functional groups. MP2D descriptors are
319 used to determine chemical similarities in the default `lazar` settings, and previous ex-
320 periments have shown, that they give more accurate results than predefined fingerprints
321 (e.g. MACCS, FP2-4).

322 *Chemistry Development Kit* (CDK, Willighagen, Mayfield, and Alvarsson (2017)) descrip-
323 tors were calculated with the PaDEL graphical interface (Yap (2011)). They include 1D
324 and 2D topological descriptors as well as physical-chemical properties.

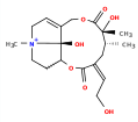
325 All investigated algorithms obtained models within the experimental variability for both
326 types of descriptors (Table 1, Table 2, Figure 1).

327 Given that similar predictive accuracies are obtainable from both types of descriptors
328 the choice depends once more on practical considerations:

329 MolPrint2D fragments can be calculated very efficiently for every well defined chem-
330 ical structure with OpenBabel (O’Boyle et al. (2011)). CDK descriptor calculations
331 are in contrast much more resource intensive and may fail for a significant number of
332 compounds (from 8290).

333 MolPrint2D fragments are generated dynamically from chemical structures and can be

Prediction:



OC=C1C[C@@H][C@C@@](C)(O)C(=O)OCC2=CC[N+](C@)2[C@H](OC1=O)CC3O)C

[PubChem](#)

Mutagenicity (Salmonella typhimurium)

Type: Classification

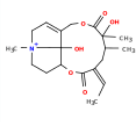
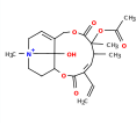
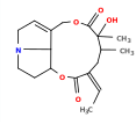
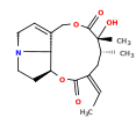
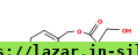
Prediction: i
mutagenic

Probability: i
non-mutagenic: 0.388
mutagenic: 0.44

Confidence:
Lower than bioassay results

Warnings:
Similarity threshold 0.2 < 0.5, prediction may be out of applicability domain.

Neighbors:

Mutagenicity (Salmonella typhimurium)		
Compound	Measured Activity i	Similarity i
	mutagenic PubChem	0.828
	mutagenic PubChem	0.447
	non-mutagenic PubChem	0.378
	non-mutagenic PubChem	0.378
	non-mutagenic PubChem	0.359

[https://lazar.in-silico.ch/predict \[-\]](https://lazar.in-silico.ch/predict [-]) ALL

Figure 7: Lazar screenshot of 12,21-Dihydroxy-4-methyl-4,8-secosenecinonan-8,11,16-trione mutagenicity prediction

334 used to determine if a compound contains structural features that are absent in training
335 data. This feature can be used to determine applicability domains. CDK descriptors
336 contain in contrast a predefined set of descriptors with unknown toxicological relevance.
337 MolPrint2D fingerprints can be represented very efficiently as sets of features that are
338 present in a given compound which makes similarity calculations very efficient. Due to
339 the large number of substructures present in training compounds, they lead however to
340 large and sparsely populated datasets, if they have to be expanded to a binary matrix
341 (e.g. as input for tensorflow models). CDK descriptors contain in contrast in every case
342 matrices with 1442 columns which can cause substantial computational overhead.

343 **Pyrrrolizidine alkaloid mutagenicity predictions**

344 Figure 2 shows a clear differentiation between the different pyrrolizidine alkaloid groups.
345 The largest proportion of mutagenic predictions was observed for Otonecines 65%
346 (407/623), the lowest for Monoesters 2% (52/1889) and N-Oxides 5% (59/1052).

347 Although most of the models show similar accuracies, sensitivities and specificities in
348 crossvalidation experiments some of the models (MPD-RF, CDK-RF and CDK-SVM)
349 predict a lower number of mutagens (2-5%) than the majority of the models (14-25%
350 (Figure 2)). lazar-CDK on the other hand predicts the largest number of mutagens for
351 all groups with exception of Otonecines.

352 These differences between predictions from different algorithms and descriptors were not
353 expected based on crossvalidation results.

354 In order to investigate, if any of the investigated models show systematic errors in the
355 vicinity of pyrrolizidine-alkaloids we have performed a detailed t-SNE analysis of all
356 models (see Figure 5 and Figure 6 for two examples, all visualisations can be found at
357 <https://git.in-silico.ch/mutagenicity-paper/figures>).

358 Nevertheless none of the models showed obvious deviations from their expected be-
359 haviour, so the reason for the disagreement between some of the models remains unclear
360 at the moment. It is however perfectly possible that some systematic errors are covered
361 up by converting high dimensional spaces to two coordinates and are thus invisible in
362 t-SNE visualisations.

363 **Conclusions**

364 A new public *Salmonella* mutagenicity training dataset with 8309 compounds was cre-
365 ated and used it to train `lazar` and Tensorflow models with MolPrint2D and CDK
366 descriptors.

367 **References**

368 Bender, Andreas, Hamse Y. Mussa, Robert C. Glen, and Stephan Reiling. 2004. “Molec-
369 ular Similarity Searching Using Atom Environments, Information-Based Feature Selec-
370 tion, and a Naïve Bayesian Classifier.” *Journal of Chemical Information and Computer*
371 *Sciences* 44 (1): 170–78. <https://doi.org/10.1021/ci034207y>.

372 Benigni, R., and A. Giuliani. 1988. “Computer-assisted Analysis of Interlaboratory
373 Ames Test Variability.” *Journal of Toxicology and Environmental Health* 25 (1): 135–48.
374 <https://doi.org/10.1080/15287398809531194>.

375 EFSA. 2011. “Scientific Opinion on Pyrrolizidine Alkaloids in Food and Feed.” *EFSA*
376 *Journal*, no. 9: 1–134.

377 ———. 2016. “Guidance on the Establishment of the Residue Definition for Dietary
378 Assessment: EFSA Panel on Plant Protect Products and Their Residues (PPR).” *EFSA*
379 *Journal*, no. 14: 1–12.

380 Hansen, Katja, Sebastian Mika, Timon Schroeter, Andreas Sutter, Antonius ter Laak,
381 Thomas Steger-Hartmann, Nikolaus Heinrich, and Klaus-Robert Müller. 2009. “Bench-
382 mark Data Set for in Silico Prediction of Ames Mutagenicity.” *Journal of Chemical*
383 *Information and Modeling* 49 (9): 2077–81. <https://doi.org/10.1021/ci900161g>.

384 Helma, Christoph, David Vorgrimmler, Denis Gebele, Martin Gütlein, Barbara Engeli,
385 Jürg Zarn, Benoit Schilter, and Elena Lo Piparo. 2018. “Modeling Chronic Toxicity: A
386 Comparison of Experimental Variability with (Q)SAR/Read-Across Predictions.” *Fron-*
387 *tiers in Pharmacology*, no. 9: 413.

388 Kazius, J., R. McGuire, and R. Bursi. 2005. “Derivation and Validation of Toxicophores
389 for Mutagenicity Prediction.” *J Med Chem*, no. 48: 312–20.

390 Maaten, L. J. P. van der, and G. E. Hinton. 2008. “Visualizing Data Using T-Sne.”
391 *Journal of Machine Learning Research*, no. 9: 2579–2605.

392 Mattocks, AR. 1986. *Chemistry and Toxicology of Pyrrolizidine Alkaloids*. Academic
393 Press.

394 O’Boyle, Noel, Michael Banck, Craig James, Chris Morley, Tim Vandermeersch, and
395 Geoffrey Hutchison. 2011. “Open Babel: An open chemical toolbox.” *J. Cheminf.* 3 (1):
396 33. <https://doi.org/doi:10.1186/1758-2946-3-33>.

397 Schöning, Verena, Felix Hamann, Mark Peinl, and Jürgen Drewe. 2017. “Editor’s
398 Highlight: Identification of Any Structure-Specific Hepatotoxic Potential of Different
399 Pyrrolizidine Alkaloids Using Random Forests and Artificial Neural Networks.” *Toxicol.*
400 *Sci.*, no. 160: 361–70.

401 Weininger, David, Arthur Weininger, and Joseph L. Weininger. 1989. “SMILES. 2.
402 Algorithm for Generation of Unique Smiles Notation.” *J. Chem. Inf. Comput. Sci.*, no.
403 29: 97–101. <https://doi.org/https://doi.org/10.1021/ci00062a008>.

404 Willighagen, E. L., J. W. Mayfield, and J. et al. Alvarsson. 2017. “The Chemistry

405 Development Kit (Cdk) V2.0: Atom Typing, Depiction, Molecular Formulas, and Sub-
406 structure Searching.” *J. Cheminform.*, no. 9(33). <https://doi.org/https://doi.org/10.1186/s13321-017-0220-4>.
407

408 Yap, CW. 2011. “PaDEL-Descriptor: An Open Source Software to Calculate Molecular
409 Descriptors and Fingerprints.” *Journal of Computational Chemistry*, no. 32: 1466–74.